J. Fluid Mech. (1977), *vol.* 82, *part* 3, *pp.* 429–448
Printed in Great Britain

A method-of-characteristics calculation of coronary blood flow

By JOHN A. RUMBERGER AND ROBERT M. NEREM
Cardio-Pulmonary Research Group, The Ohio State University, Columbus

(Received 5 August 1976 and in revised form 10 January 1977)

The one-dimensional unsteady flow equations for flow in an elastic tube have been solved by employing the method of characteristics and used to predict the development of the flow and pressure wave forms in the left coronary artery system of the horse. Input data to this model include *in vivo* measurements of wave speed and aortic-root pressure, both of which were carried out in horse experiments. In addition, estimates of vessel taper and fluid losses due to branching were established from plastic casts of the horse coronary arteries and from *in vivo* flowmeter data. The calculated results have confirmed earlier experiments in revealing a relatively large systolic component of flow in the major epicardial vessels. However, the calculations indicate that, once within the myocardium, the systolic flow component quickly diminishes and the diastolic flow component becomes increasingly important. The pressure pulse does not peak as observed in the aorta, but rather rounds out with systolic pressures decreasing slowly and diastolic pressures decreasing more rapidly with distance from the coronary ostium. The presence of relatively large amplitude, low frequency waves (of the order of 5–10 Hz), which were observed mainly during diastole in horse experiments, has also been confirmed by the computer calculations. Similar calculations carried out for conditions simulating the dog and human coronary systems indicate that such oscillations become higher in frequency and lower in amplitude with decreasing animal size.

1. Introduction

The development of an adequate description of the detailed fluid-dynamic characteristics of the coronary circulation has been impeded by the general inaccessibility and small diameter of the coronary vessels in most animals and by limitations on instrumentation size. This has been true even for the superficial (extramural) vessels which lie on the surface of the heart muscle. Recently, however, point velocity measurements in the coronary arteries have been carried out in horses using both hot-film anemometer (Nerem *et al.* 1976) and pulsed ultrasonic Doppler velocity meter (PUDVM) (Wells *et al.* 1977) systems. Horses have been chosen for these studies of coronary blood flow owing to the large artery diameters available (up to 1·5 cm for the left common coronary artery) and their proved stamina to withstand detailed cardiac investigations.

Results obtained in studies using a constant-temperature hot-film anemometer system have revealed that, downstream of the entrance (ostium) to the left common coronary artery, the velocity profile is skewed towards the outer wall. In this region the

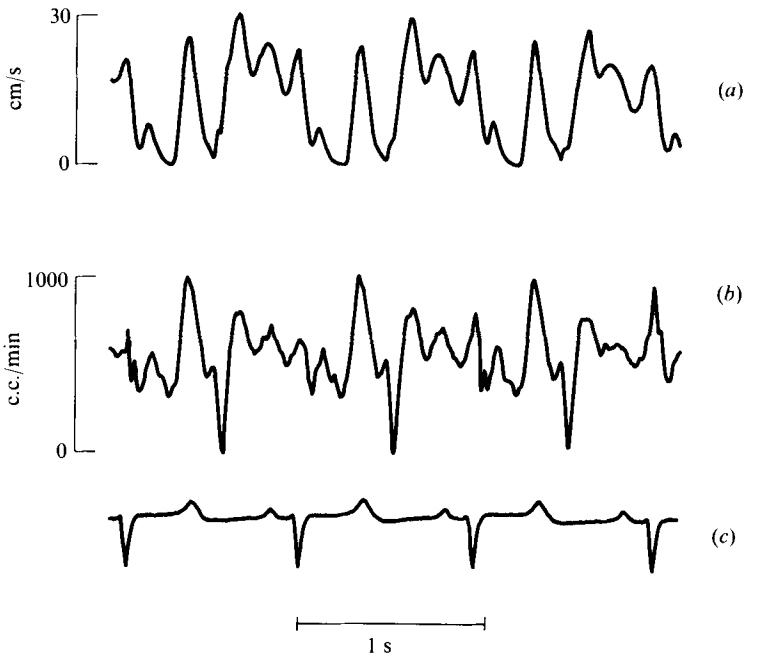

FIGURE 1. Simultaneously measured (*a*) centre-line velocity wave form and (*b*) electromagnetic flowmeter wave form together with (*c*) ECG for left anterior descending coronary artery in an anaesthetized horse.

left common coronary artery is curving over the base of the heart, and thus this skewing is as would be expected for fully viscous flow in a curved tube. As one proceeds further downstream, the left common coronary artery then bifurcates (at a point 3–4 cm from the ostium for a large horse) to form its first major branches: the left anterior descending (LAD) and left circumflex coronary arteries. Measurements just downstream of this bifurcation in general reveal profile skewing to be away from the flow divider in both branches. This suggests that the secondary flow effects associated with the curvature of the plane of bifurcation (as the arteries curve over the base of the heart) may dominate the normal bifurcation effects on the velocity pattern. Further downstream, e.g. 5–6 diameters past the point of bifurcation, hot-film anemometer results do indicate that the velocity profile has become relatively fully developed and, at least on an instantaneous basis, resembles that of Poiseuille flow.

In spite of the somewhat detailed results summarized above, there still exist many characteristics of coronary blood flow that remain unquantified. This is particularly true with regard to pressure wave form development, wave transmission characteristics and the significance of wave reflexion phenomena. Of particular fluid-mechanical interest has been the observation of relatively large amplitude, low frequency oscillations in velocity (obtained with pulsed ultrasonic Doppler, hot-film anemometry and electromagnetic flowmeter systems) and pressure. These have a frequency of the order of 5–10 Hz and are observed to be superimposed upon the basic coronary flow and pressure wave forms measured in the extramural vessels of the horse (see figure 1). Velocity profile measurements in these regions using a hot-film anemometer system

have revealed these oscillations to exhibit no radial dependence of phase, thus apparently ruling out vortex shedding as a possible mechanism.

Obviously, an *in vivo* experimental study of this oscillation phenomenon under varying physiological conditions would be desirable from many viewpoints. However, owing to the limited number of sites conveniently available for investigation experimentally, an overall picture of *in vivo* coronary flow and pressure development based on animal measurements is not possible. It is thus the purpose of this investigation to develop a mathematical treatment of coronary blood flow that qualitatively and, as far as possible, quantitatively reproduces the salient features of coronary blood flow as observed *in vivo*. Of particular interest will be the use of this model to study the characteristics of the pressure and flow oscillations previously noted.

2. Coronary dynamics and a model for coronary blood flow

Coronary blood flow is biphasic, exhibiting two minima and two maxima during each cardiac cycle. During the ejection phase of the heart cycle (systole), blood is ejected into the coronary artery via inlets (ostia) which originate at the root of the aorta. In the extramural vessels near the ostia this systolic component of blood flow has been found to be as much as one-third of the total flow occurring during the cardiac cycle (see figure 1). However, in the more distal vessels which eventually penetrate deep into the heart muscle itself, the blood flow during systole is severely attenuated. This is due to the large increase in compressive stress which is developed in the heart wall at this time and the attendant increase in resistance to flow. During diastole (the resting phase of the heart cycle), the resistance to flow decreases quickly and an additional surge of blood is observed in all sections of the coronary artery system. The nature of this extravascular compression on the left coronary blood vessels has been observed to follow approximately the time development of the left ventricular pressure (Kirk & Honig 1964; Randall & Armour 1971), although the distribution of this stress across the left ventricular wall has not been adequately determined. However, the data of Kirk & Honig (1964), Randall & Armour (1971) and Rubio & Berne (1975), though not in total agreement, suggest that it is maximal in the subendocardial layers (those adjacent to the left ventricular chamber) and minimal in the subepicardial layers (near the exterior surface of the heart).

The pressure wave form development in the left extramural coronary arteries of the horse is illustrated in figure 2. In general, the pressure pulse at the left ostium is identical to the aortic-root pressure. However, as was noted earlier, further downstream from the ostium relatively large amplitude, low frequency oscillations (of the order of 5–10 Hz) are observed to occur. These are particularly noticeable during the latter portion of the cardiac cycle and become progressively more prominent as one proceeds distally. Furthermore, the dicrotic wave or incisura, observed about midway into the cycle in the aortic and ostium pressure wave forms, is slowly masked by these oscillations as one proceeds downstream.

There are numerous factors which must be taken into account in the development of an adequate mathematical model of coronary blood flow. Obviously the time dependence of the flow must be considered. Another factor, however, is the suggestion from *in vivo* measurements (Rumberger, Nerem & Muir 1977) that the propagation speed of small pressure waves through the coronary system is highly dependent on the local

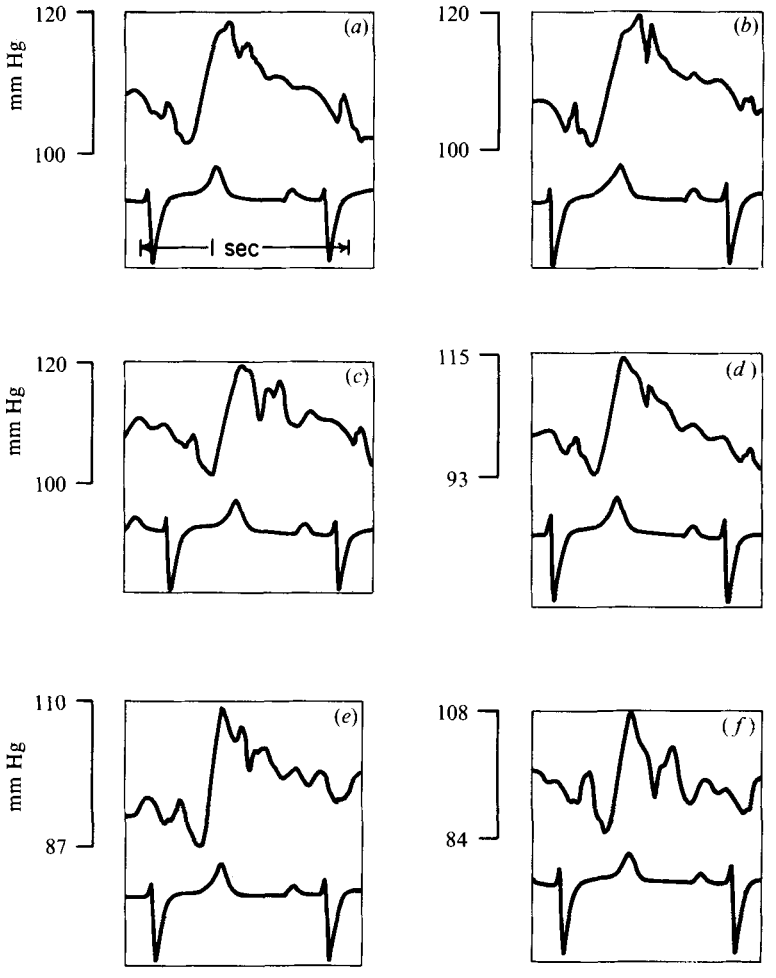

FIGURE 2. Temporal *in vivo* pressure wave forms at various distances from the left coronary ostium in an anaesthetized horse. (*a*) Aortic 120/100 at 1 cm. (*b*) Aortic 120/100 at 3 cm. (*c*) Aortic 120/100 at 5 cm. (*d*) Aortic 115/95 at 7 cm. (*e*) Aortic 110/95 at 9 cm. (*f*) Aortic 110/90 at 12 cm.

pressure as well as on distance from the ostium. The numerous branches occurring along the actual artery system and the associated fluid losses must also be considered. In addition, fluid friction, the time dependence of the artery cross-sectional area, and the extravascular compression of the more distal blood vessels are effects which need to be incorporated into any realistic model. Although blood in the larger arteries may be approximated as a Newtonian fluid, some of the other effects are intrinsically nonlinear.

Several different types of mathematical model have been employed to study arterial blood flow. Among these have been the pure-resistance or steady-state perfusion models, the lumped-parameter or 'Windkessel' models and linear models of the type developed by Womersley (1957) and McDonald (1974). None of these approaches offers quantitatively the features desired here since they do not account for nonlinear flow and wave propagation effects.

Ling *et al.* (1973) and Atabek, Ling & Patel (1975) have developed a two-dimensional nonlinear model of blood flow which is capable of predicting the mean flow, as well as velocity profiles, across a given artery section and which has been applied to both the dog aorta and the coronary arteries. However, an *in vivo* measurement of the pressure gradient in the vessel section is necessary as input data. This makes the model unsuitable for predicting flow in vessels where a prior knowledge of the pressure gradient is not available. Furthermore, it is difficult, if not impossible, to apply this method to an entire vascular system such as that of interest here.

Another technique available for the prediction of arterial blood flow is through the use of the method of characteristics to solve the nonlinear, one-dimensional, unsteady equations of motion. This method is an attractive one for this investigation since it intrinsically accounts for forward- and backward-running waves at each site in the physical plane. In using the one-dimensional equations, the pressure and flow are considered to be a function of only one spatial co-ordinate, i.e. distance along the vessel. Although such a one-dimensional model is in some ways more approximate than the two-dimensional linear models noted earlier, the effects of nonlinear wave propagation and vessel branching, which are at least equally important, may be easily included.

Rockwell (1969) used the method of characteristics to solve the equations for a one-dimensional model of aortic blood flow which included a pulse wave velocity which was a function of both pressure and distance from the aortic valve and fluid volume losses due to vessel branching. By specifying distal and proximal boundary conditions, Rockwell calculated the flow and pressure wave form development from the aortic valve to points as far distal as the abdominal aorta. Features such as the steepening of the aortic pressure wave form as one proceeds downstream of the valve were predicted and found to confirm *in vivo* results (McDonald 1974). Womersley's (1957) original linear model failed to predict this, and Rockwell's results thus have established the importance of nonlinear effects in modelling arterial flow.

Van der Werff (1974) also used the method of characteristics to study aortic blood flow, but with a statement of only proximal boundary conditions (here both the input pressure and the flow wave forms are required) and employing the fact that the solution is periodic. The major limitations of this method are that it does not allow systematic examination of the effect of altered downstream boundary conditions on the development of pressure and flow wave forms and thus that any altered condition to be studied must first be produced in the laboratory so as to have available the appropriate proximal boundary conditions for the calculation.

On the basis of the success of Rockwell (1969) and Van der Werff (1974), the method of characteristics has been chosen for use in solving the system of equations resulting from the model to be used here. The blood is assumed so be an incompressible Newtonian fluid whose motion can be adequately described as unsteady and one-dimensional in nature. The vessel is assumed to be a straight but tapered elastic tube, which allows for a continuous seepage of fluid through its walls to simulate losses due to branching. The radial inertia of the tube and the fluid is neglected and the effects of wall friction are accounted for only in an approximate manner. The elastic properties of the vessel are prescribed through specification of the propagation speed of small pressure waves through the system and the dependence of this wave speed on transmural pressure and spatial location. The heart muscle is assumed to be a thick-walled structure with the blood vessel in question running from the base to the apex of the left

heart, initially lying extramurally but, with distance from the left coronary ostium, becoming slowly encompassed by the left ventricular myocardium. The extravascular compressive stress, which is developed within the myocardium during systole and which acts directly upon the periphery of the vessel, is assumed to be governed by the development of the left ventricular pressure.

3. Development of the characteristic equations

The motion of blood in the coronary system is treated here as being governed by the unsteady one-dimensional continuity and momentum equations and by a relationship between the vessel cross-sectional area and pressure. These equations are as follows:

$$\frac{\partial S}{\partial t}+\frac{\partial (VS)}{\partial z}+\psi = 0, \tag{1}$$

$$\frac{\partial V}{\partial t}+V\frac{\partial V}{\partial z}+\frac{1}{\rho}\frac{\partial P}{\partial z}=f, \tag{2}$$

$$S = S(\eta, z). \tag{3}$$

$V(z,t)$ denotes the instantaneous flow velocity (averaged across the vessel), $P(z,t)$ the local pressure (referenced to atmospheric), ψ the rate of volumetric outflow per unit length of the vessel (due to flow into small branch vessels) and f the force per unit mass representing the effect of wall friction. Both ψ and f are left unspecified at present. η is the transmural pressure acting on the vessel, i.e. the stress acting perpendicular to the vessel wall, and is equal to the difference between the internal blood pressure and the extravascular compressive stress developed within the left ventricular myocardium. This compressive force is assumed to act uniformly about the circumference of the blood vessel.

It also is assumed that $\eta = \eta(z,t)$, where the spatial dependence is due to the extravascular compression. This effect is minimal in the extramural vessels and maximal in the subendocardial vessels adjacent to the left ventricular chamber. The time history of this stress is assumed to follow the left ventricular pressure development $P_v(t)$. On the basis of the assumption that the effects of distance z and time t are separable, η is here expressed as

$$\eta = P-\xi(z)\,P_v(t), \tag{4}$$

where the functional form of ξ must be known *a priori* but is left unspecified for the moment.

Equations (1)–(3) represent a set of three equations in three unknowns, V, P and S. Using (3), S may be eliminated as a dependent variable. Using (3) and the functional form of η provided by (4), substitution into (1) yields [assuming $P_v \neq P_v(z)$]

$$\frac{\partial S}{\partial \eta}\bigg|_z\left[\frac{\partial P}{\partial t}-\xi(z)\frac{dP_v}{dt}\right]+S\frac{\partial V}{\partial z}+V\frac{\partial S}{\partial \eta}\bigg|_z\left[\frac{\partial P}{\partial z}-P_v\xi'(z)\right]+V\frac{\partial S}{\partial z}+\psi = 0. \tag{5}$$

Using L_1 to denote (2) and L_2 to denote (5) and considering the linear combination $L = L_1+\lambda L_2$, where λ is an undetermined multiplier, gives

$$L = \left[\frac{\partial V}{\partial t}+\frac{\partial V}{\partial z}(V+\lambda S)+\lambda\frac{\partial S}{\partial \eta}\bigg|_z\left[\frac{\partial P}{\partial t}+\frac{\partial P}{\partial z}\left(V+\frac{1}{\rho\lambda(\partial S/\partial\eta)_z}\right)\right]\right]$$
$$-\lambda\frac{\partial S}{\partial \eta}\bigg|_z\xi\frac{dP_v}{dt}+V\xi'(z)\,P_v+\lambda V\frac{\partial S}{\partial z}\bigg|_\eta+\lambda\psi-f = 0. \tag{6}$$

If $V = V(z, t)$ and $P = P(z, t)$ and the chain rule for ordinary differentials is used, then from (6)

$$dz/dt = V + \lambda S = V + \frac{1}{\rho\lambda(\partial S/\partial\eta)_z}. \tag{7}$$

Setting $\lambda = \pm c/S$, it follows that

$$c = \left(\frac{S}{\rho(\partial S/\partial\eta)_z}\right)^{\frac{1}{2}}. \tag{8}$$

dz/dt is the slope of the characteristic lines (of which there exist two for hyperbolic partial differential equations such as L). There are thus two separate ordinary differential equations of first order. For dz/dt these define two one-parameter families of characteristic curves in the z, t plane which belong to the solutions for $P(z, t)$ and $V(z, t)$ and which form a curvilinear co-ordinate net. By restricting the application of (6) to characteristic lines for which the equation for dz/dt holds, it follows that

$$dz/dt = V \pm c, \tag{9}$$

$$\frac{dV}{dt} \pm \frac{1}{\rho c}\frac{dP}{dt} - f \pm \frac{cV}{S}\frac{\partial S}{\partial z}\bigg|_\eta \pm \frac{c\psi}{S} \pm \frac{1}{\rho c}\left[\xi(z)\frac{dP_v}{dt} + V\xi'(z)P_v\right] = 0. \tag{10}$$

Here the wave speed of a small disturbance in the fluid is defined by a characteristic line whose slope dz/dt equals $V + c$ at any point K on that characteristic. Therefore, in (8), c is the local speed at which small disturbances travel relative to the fluid. In the case of a blood vessel, c is the local wave speed and is itself, for a distensible artery, a function of transmural pressure and location, i.e. $c = c(\eta, z)$.

Intrinsic within this formulation and the application of the method of characteristics to the present problem is the assumption that certain geometric and mechanical relationships are known *a priori* for the coronary arteries. In particular, the solution of the problem can be initiated only once the functional forms of the wave speed dependence $c = c(\eta, z)$ and the cross-sectional area relationship $S = S(\eta, z)$ are specified. Furthermore, the outflow function ψ, the friction expression f and the transmural pressure η must be expressed as explicit functions of $(P, V; z, t)$, together with appropriate initial and boundary conditions.

It should be noted that coronary flow dynamics are governed by numerous mechanical, geometrical and neural factors. Thus the present model, in incorporating only a group of the known mechanical factors influencing coronary blood flow, should not be expected to yield a complete picture of coronary haemodynamics. Likewise, no single set of mechanical parameters will serve to describe the salient features observed in all *in vivo* measurements. Nevertheless, on the basis of *in vivo* experiments performed in our laboratory, a standard computer model (SCM) with its own particular set of governing parameters has been prescribed and is used here to investigate the development of the pressure and flow wave forms in the left coronary arteries of the horse. The input to the SCM, based on our experimental measurements, is discussed in the next section.

4. Input to standard computer model from experiments

Wave speed and cross-sectional area

Measurements of the propagation characteristics of small pressure waves in the extramural coronary vessels of anaesthetized horses (Rumberger *et al.* 1977) have suggested

that the wave speed c (m/s) is highly dependent on the intralumenal pressure P (mm Hg) and on the distance z (cm) from the left coronary ostium. Using the method of least squares, a polynomial curve fit to these data was found to yield a linear dependence of the form

$$c(P,z) = 1{\cdot}57 + 0{\cdot}0363P + 0{\cdot}125z. \tag{11}$$

Assuming that the pressure dependence in the subepicardial and subendocardial vessels is now reflected in the transmural pressure development, the wave speed dependence in the coronary arteries of the horse was assumed to be given by the expression

$$c(\eta,z) = A + B\eta + Dz. \tag{12}$$

The actual values used as input to the standard computer model (SCM) are

$$A = 1{\cdot}57\,\text{m/s}, \quad B = 0{\cdot}0363\,\text{m/s mm Hg} \quad \text{and} \quad D = 0{\cdot}08\,\text{s}^{-1}.$$

Substituting (11) into (8) and integrating gives

$$S = A(z)\exp\left(\frac{\eta-\eta_0}{\rho c(\eta,z)\,c(\eta_0,z)}\right), \tag{13}$$

where η_0 is a reference pressure and $A(z)$ is the cross-sectional area dependence on z for $\eta = \eta_0$. Using fibreglass casts made from excised horse hearts at a perfusion pressure of $\eta_0 = P_0 = 100$ mm Hg, it was found that the cross-sectional area of the artery (following the left common/left anterior descending artery combination) could be approximated by a decreasing exponential of the form

$$A(z) = S(\eta_0,z) = S_0(\eta_0)\,e^{-\beta z}. \tag{14}$$

Here $S_0(\eta_0)$ is the cross-sectional area of the left common coronary artery at the ostium at a pressure of 100 mm Hg. Thus, upon substitution (13) becomes

$$S(\eta,z) = S_0(\eta_0)\exp\left(-\beta z + \frac{\eta-\eta_0}{\rho c(\eta,z)\,c(\eta_0,z)}\right). \tag{15}$$

In order to obtain a better fit to the area measured from the fibreglass casts, three separate exponentials corresponding to three different regions of the coronary system to be studied were used:

$$S(\eta,z) = \begin{cases} 1{\cdot}5\exp\left(-0{\cdot}225\,z + \dfrac{\eta-100}{\rho c(\eta,z)\,c(100,z)}\right), & 0 < z < 3\,\text{cm}, \\ S(\eta,3)\exp\left(-0{\cdot}125\,(z-3) + \dfrac{\eta-100}{\rho c(\eta,z)\,c(100,z)}\right), & 3 < z < 12\,\text{cm}, \\ S(\eta,12)\exp\left(-0{\cdot}151(z-12) + \dfrac{\eta-100}{\rho c(\eta,z)\,c(100,z)}\right), & 12 < z < 50\,\text{cm}. \end{cases} \tag{16}$$

In all three of these equations S has the units cm^2.

Friction expression

The frictional force per unit mass at the artery wall acting upon a vessel circular in cross-section and of radius $(S/\pi)^{\frac{1}{2}}$ is given by

$$f = \frac{2}{\rho}\left(\frac{\pi}{S}\right)^{\frac{1}{2}}\tau_w. \tag{17}$$

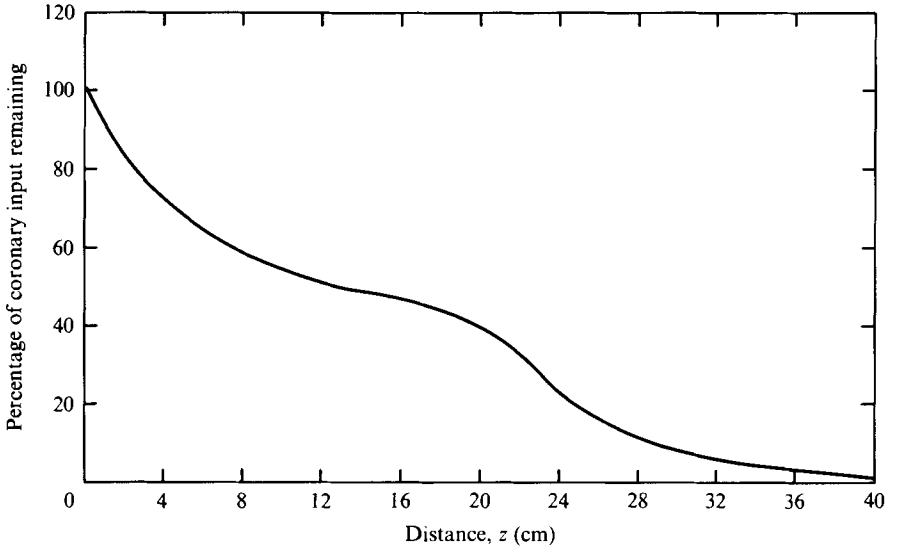

FIGURE 3. Amount of blood remaining in left common/LAD coronary artery as a percentage of total input *vs.* distance from the left coronary ostium obtained from estimates of branching from polyester-resin cast of coronary arteries.

Here τ_w is the frictional shearing stress at the wall. The magnitude of this shear stress is a flow-dependent quantity which has not been adequately described *in vivo* for any major blood vessel, let alone the coronary arteries. However, from *in vivo* velocity profile measurements using a hot-film anemometer probe in the major extramural vessels of the horse (Nerem *et al.* 1976), it has been shown that the velocity profile rapidly approaches an almost fully developed, though skewed character within a few vessel diameters distal to the left ostium and, although time varying, at any instant of time is not totally unlike that of Poiseuille flow. Since it is only the average effect of the profile on the velocity wave form development that is of interest here, it was felt that a laminar Poiseuille type of friction expression would be adequate to describe the viscous forces. Using Poiseuille's law it follows that

$$f = \frac{-8\mu V}{\rho}\frac{\pi}{S}. \tag{18}$$

For input to the SCM the fluid density ρ was assumed to equal 1·055 g/c.c. and the viscosity coefficient μ to equal 0·0365 P.

Outflow expression

The outflow of blood from the left common/left anterior descending artery is modelled by a continuously distributed seepage which is defined by the function ψ. For the coronary arteries the loss of fluid from the main artery to branches must be a function of the perfusion pressure difference existing between the vessel and the capillary bed, $P - P_c$ (where P_c is the capillary pressure), as well as of the relative distribution of branch vessels and the size of each compared with the main artery dimensions. In addition, the cyclic compression of the small myocardial arteries must be taken into account.

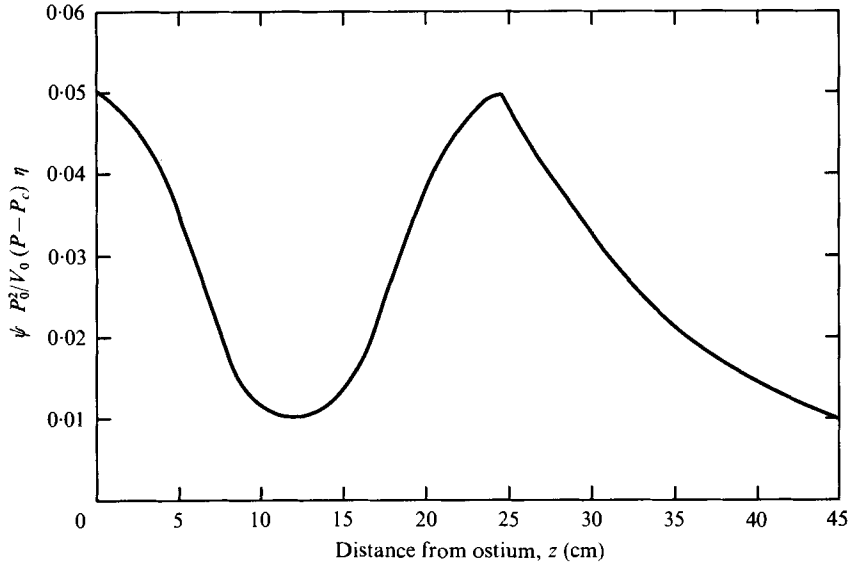

FIGURE 4. Quasi-steady outflow distribution used as input to method-of-characteristics computer program. $Q = 0{\cdot}03$ cm^{-1}, $R = 0{\cdot}02$ cm^{-1}.

Owing to the large number of branches emanating from the left common and left anterior descending arteries, the specification of discrete fluid losses is not possible. However, one may make a crude estimate of the outflow distribution using fibreglass casts made of the coronary system of the horse prepared specifically for this purpose. By estimating fluid losses to branch vessels on the basis of the ratios of the areas of the main artery and the daughter branch as obtained from the casts, the distribution of the amount of fluid remaining in the main artery (as a percentage of the total left coronary inflow) has been derived and is shown in figure 3. The rate of vessel seepage per unit length is given by the slope of this distribution and is shown graphically for the SCM in figure 4. Among the various forms considered, the one judged most realistic in terms of the final computer results was

$$\psi = \begin{cases} V_0 \dfrac{(P-P_0)\eta}{P_0^2}\left(Q + R\cos\dfrac{2\pi z}{24}\right), & z \leqslant 24 \text{ cm}, \\ V_0 \dfrac{(P-P_0)\eta}{P_0^2}(Q+R)\,e^{-K(z-24)}, & z > 24 \text{ cm}. \end{cases} \tag{19}$$

For the SCM, K equals $-0{\cdot}07$ cm^{-1}, Q and R equal $0{\cdot}03$ cm^{-1} and $0{\cdot}02$ cm^{-1} respectively, and ψ is in cm^2/s. V_0 (equal to 700 c.c./min for the SCM) is the total inflow through the left ostium, P_0 (equal to 100 mm Hg) the perfusion pressure used for the preparation of the fibreglass casts and P_c the capillary pressure. The ratio η/P_0 accounts for the cyclic compression of the vessel by the heart muscle.

Even though these expressions are admittedly crude, until more detailed information on discrete branching effects is available it is felt that the approach taken here is reasonable.

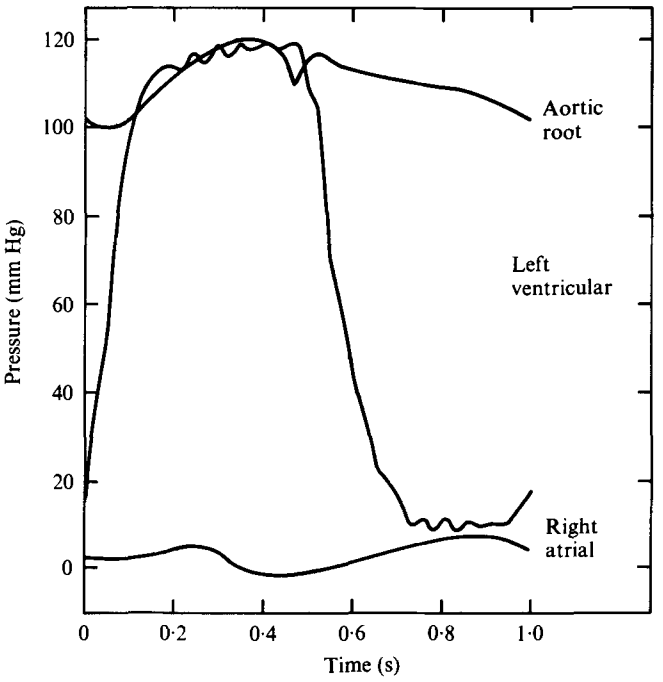

FIGURE 5. Pressures used as input to method-of-characteristics computer program.

Transmural pressure

The distribution $\xi(z)$ of the intramyocardial stress across the left ventricular wall was modelled by an exponential function with the result that the transmural pressure η has the form

$$\eta(z,t) = P - \gamma(1 - e^{-\phi z})\, P_v. \tag{20}$$

For the SCM, ϕ has been set equal to 0·072 and γ to 0·9. Use of such a form for the extravascular compression was found to produce the most realistic results when compared with experiments (see discussion).

Initial conditions

For the calculations to be presented here, the initial pressure and flow values at time $t = t_0$ were assumed to decrease exponentially with distance from the ostium. The entrance values, i.e. at the ostium, were determined from *in vivo* experiments on horses. Since the numerical integration of the equations continues through several cardiac cycles, during which the effects of this initial distribution on the final solution are lost, it is not necessary to be particularly accurate in specifying these initial values. In fact, various forms for these initial conditions were used and found to have a negligible effect on the final solution.

Boundary conditions

Unlike the initial conditions, an accurate specification of the boundary conditions at both ends of the blood vessel which is valid for all time is extremely important. In principle, either the input flow rate or pressure may be specified as a function of time

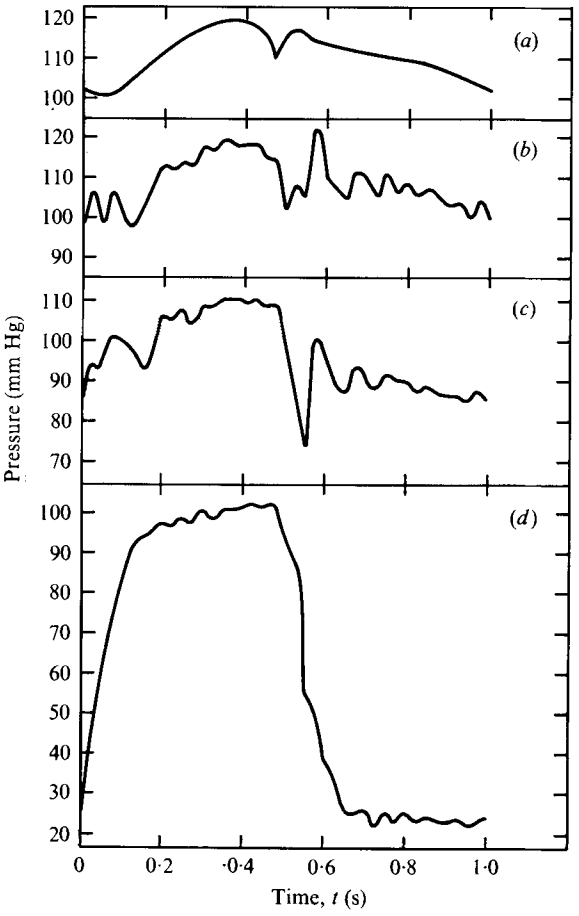

FIGURE 6. Temporal left coronary pressure at various distances from the left coronary ostium for the standard computer model. (*a*) $z = 0$, (*b*) $z = 15$ cm, (*c*) $z = 30$ cm, (*d*) $z = 45$ cm.

at the proximal boundary. However, owing to the numerous pressure recordings available from our laboratory for the coronary arteries and the observation that the left ostial pressure wave form is identical to that of the aortic root, it was the aortic pressure that was actually chosen as the proximal boundary condition.

Equally allowable in the formulation of the problem is the specification of either the distal flow or pressure as a downstream boundary condition. However, intralumenal values of neither of these haemodynamic variables are available for use as a distal boundary condition. In choosing pressure as a condition, one thus is forced to conjecture on actual capillary bed values, and for the present calculations a right atrial pressure wave form (obtained from a dog) was used as the distal boundary condition. Since the venous pressure drop is small, it is a perfusion pressure difference equal to the local pressure minus the right atrial pressure that governs the flow, ignoring the effects of right ventricular compression. The justification for using this pressure is debatable; however, until such time as the pressure levels in the capillary bed at the heart apex become measurable, it is felt to be a reasonable approximation.

Though actually not a boundary condition on the equations, the left ventricular pressure and its time derivative are important in governing the extravascular com-

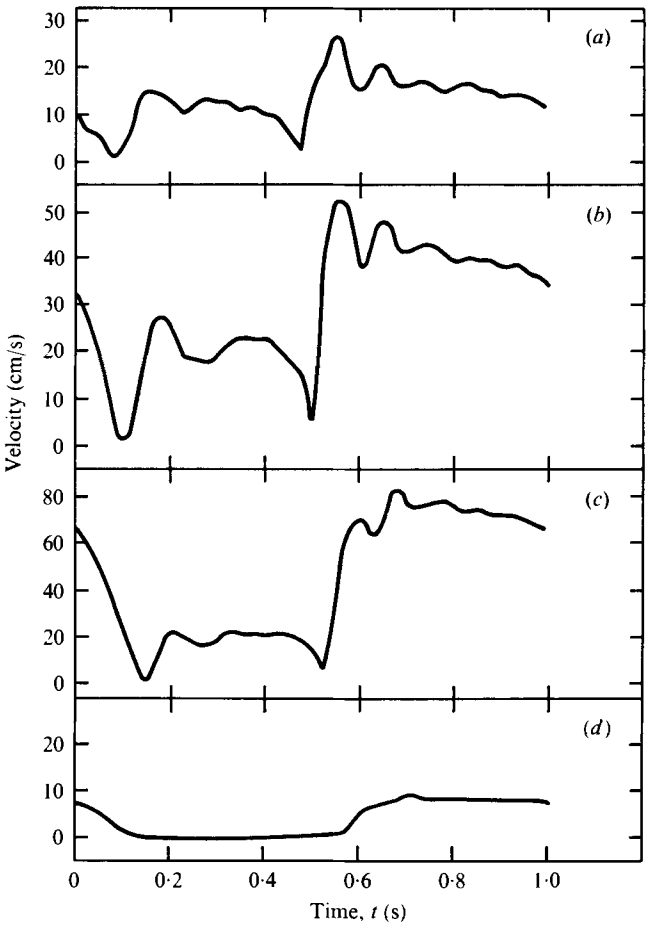

FIGURE 7. Temporal left coronary blood flow velocity at various distances from the left coronary ostium for the standard computer model. (*a*) $z = 0$, (*b*) $z = 15$ cm, (*c*) $z = 30$ cm, (*d*) $z = 45$ cm.

pressive-stress development. This in turn affects the outflow through branch vessels, the local cross-sectional area and the wave speed, which is a function of the transmural pressure. Thus, for each *in vivo* experiment, values of the aortic-root and left ventricular pressure were measured. The left ventricular and boundary-condition pressure wave forms used for the standard computer model are shown in figure 5. These were entered into the computer model using a 24 term Fourier series.

5. Results and discussion for standard computer model

The characteristic equations (8) and (9) were solved by replacing them by their forward-difference equivalents and solving by the method of specified time intervals as discussed by Lister (1960). The computing mesh sizes used were $\Delta z = 1$ cm and $\Delta t = 0{\cdot}001$ s with T, the period of one cardiac cycle, set equal to 1 s. A total of two iterations (two complete cycles) was sufficient to produce the steady-state solution. Successive iterations were found to differ by less than 1 % from the flow and pressure results for two iterations. To examine further the accuracy of the numerical inte-

gration, several computer runs were performed with $\Delta z = 0{\cdot}05$ cm and $\Delta t = 0{\cdot}0005$ s. However, essentially no difference could be detected in the steady-state results after two iterations when comparing solutions for both mesh sizes.

Flow and pressure results are not presented here for locations below the point corresponding to $z = 45$ cm, even though the terminal distance was set at $z = L = 50$ cm. This is because at $z = L$ the downstream boundary condition was specified as a right atrial pressure wave; this condition was assumed and does not necessarily represent the correct distal value for the pre-capillary bed pressure.

Figure 6 presents representative results for pressure wave forms at various distances from the ostium obtained using the SCM. These reveal the presence of a wave oscillation – prevalent mainly during diastole – which masks the incisura within a distance of a few centimetres from the ostium. This is in qualitative agreement with the trends presented in figure 2 and with those in general demonstrated by the *in vivo* experimental results previously discussed. It should be noted that, at the most distal arterial sections, the pressure wave form is identical in shape (but not in magnitude) to the left ventricular pressure. Although confirmation of this through *in vivo* experiments is not possible at present, it is reasonable and to be expected considering that the extravascular compression must be reflected within the easily distensible deep myocardial vessels.

Figure 7 presents results of the SCM for the coronary flow velocity at various distances z from the ostium. The flow oscillations are seen to be reproduced qualitatively in those curves corresponding to extramural vessels ($0 \leqslant z < 20$ cm), but are predicted gradually to diminish in prominence until they are completely attenuated in the areas corresponding to deep myocardial positions (e.g. at $z = 45$ cm). In addition, the relative contribution of systole to the total flow occurring during the cardiac cycle is predicted to decrease with increasing distance from the ostium, as has been indicated qualitatively by others. This is due to the compression of the vessels and thus the significantly increased flow resistance which occurs during systole in the myocardial regions.

The major emphasis of the discussion up to this point has been on qualitative comparisons between theory and experiment. However, it is also of interest to evaluate this model from a quantitative viewpoint, both in order to judge the validity of the formulation as well as to establish areas where further refinements in the model are necessary. In this context it should be noted that wide differences in coronary blood flow patterns have been observed experimentally in different animals. Consequently, one should not expect too much in comparing *in vivo* experimental results with the results of the idealized computer model. However, by using the *in vivo* aortic and left ventricular pressures of several animals for whom volumetric flow measurements also were available (obtained using electromagnetic flow cuffs), quantitative comparisons between experimental and computer results have been carried out and are presented in figures 8 and 9. Here the ordinate is the instantaneous mean flow velocity $V = Q/S$, where Q is the volumetric flow rate and S is the cross-sectional area. The calculations presented reveal qualitatively the same wave form patterns during systole as have been measured, although the amplitudes are somewhat different. During diastole the computer calculations are seen to compare quantitatively quite favourably with experiment. The total flow (integrated across the entire cardiac cycle) for the measured and the computed wave forms is approximately the same in both figure 8 and figure 9,

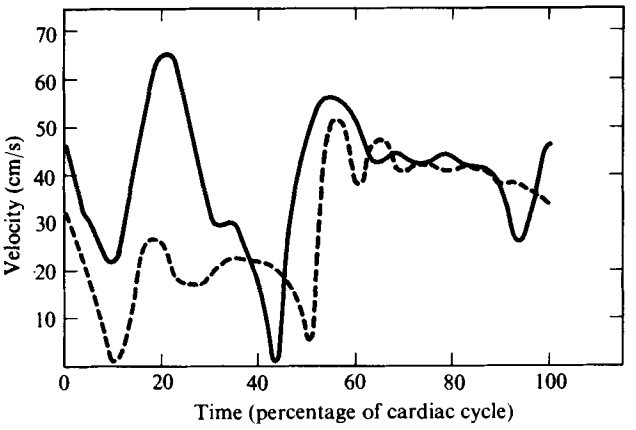

FIGURE 8. Comparison of *in vivo* flow velocity $V = Q/S$ from a horse at 15 cm distal to the left coronary ostium (solid curve) and the standard computer model for $z = 15$ cm (broken curve).

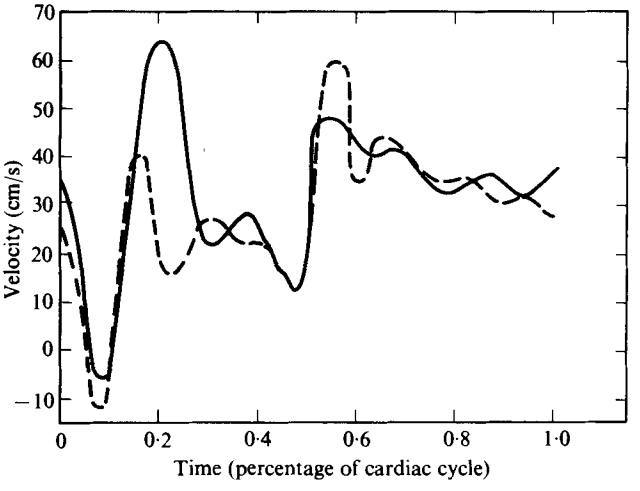

FIGURE 9. Comparison of *in vivo* flow velocity $V = Q/S$ from a horse at 15 cm distal to the left coronary ostium (solid curve) and the standard computer model for $z = 15$ cm (broken curve).

even though the systolic peak flow velocities are calculated here to be nearly half those observed in the experiments. Furthermore, the predicted amplitude and frequency of the flow oscillations, which occur mainly during diastole, are seen to compare quite favourably.

Thus the general characteristics of *in vivo* coronary flow patterns are reproduced well with the exception that the systolic flow rates are noticeably in error. This suggests that the systolic phase is the more difficult period of the cardiac cycle to model explicitly. One weakness of the present formulation might be the modelling of the compression of the blood vessels, particularly as it applies during the systolic phase of the cycle. Certainly a more accurate form for the time development of this myocardial stress could lead to a better reproduction of the systolic volume flow time history. However, up to the present it has not been possible to measure *in vivo* the time development of this extravascular compression. The outflow function ψ or the functional form of the transmural pressure η might also be the cause of the quantitative differences

observed during systole. However, various modifications to these two parameters have failed to improve the prediction of systolic flow; and it appears that more detailed experimental information on cardiac dynamics will be necessary before any further significant improvements in this model can be made.

With regard to the flow oscillations observed during diastole, Wells *et al.* (1977) have reported similar observations in their pulsed ultrasonic Doppler experiments on the left coronary arteries of the pony. They conjectured that these perturbations of the flow velocity could be caused by the vibratory motion of the blood vessels in response to stress waves travelling across the heart muscle during left ventricular contraction. In this case the velocity signals recorded would represent a superposition of a coronary flow signal associated purely with the fluid dynamics of the system and locally induced flow components associated with motion of the vessels themselves. However, the fact that these oscillations are quantitatively reproduced quite well by the SCM (which does not include the response of the blood vessels to the vibratory movement of the heart mass during contraction) tends to preclude the possibility of stress waves being primarily responsible for the occurrence of the oscillatory, wavelike phenomena. The results suggest, rather, that the flow and pressure wave forms in the left coronary arteries must be highly dependent on the nature of the wave reflexions occurring continuously within the system. This is just as was concluded by Rockwell (1969) for the aorta.

It should be noted that there is evidence that the nature of these oscillations may be size (or species) dependent. Though the results of Wells *et al.* (1977) confirm the *in vivo* data presented here from a qualitative viewpoint, quantitatively their results on 200 kg ponies do not compare with the results from our studies on 500 kg horses. In even smaller animals, owing possibly to poor fidelity of the flow measurement devices, these oscillations have not been universally observed. For example, flow traces taken in the left anterior descending coronary artery of 15 kg dogs in our own laboratory are devoid of these flow oscillations, yet a recent measurement in a 35 kg Great Dane provided evidence of them. The results of Atabek *et al.* (1975) from coronary arteries of larger dogs indicate a developing flow oscillation activity. Furthermore, the results of Gregg, Khouri & Rayford (1965) in the left circumflex coronary artery of a conscious dog show a quite distinct wavelike motion to be present on flow traces during diastole. These waves, however, appear to be of a higher frequency (10–20 Hz) and lower amplitude than those calculated using the computer model and those observed *in vivo* in the horse. In addition, results on coronary flow patterns in dogs obtained using catheter tip flowmeters in the laboratory of Peiper (1976, private communication) at the Ohio State University have indicated qualitatively the same character of wave oscillation activity as is exhibited by the results of Gregg *et al.* (1965).

To examine this further, a series of parametric calculations was carried out. These have been used to study more closely the importance of the governing mechanical parameters in the flow and pressure wave form development. From this the effects of altered outflow on the computed flow wave forms were found to be of little consequence except in extreme cases. As for the effects of an altered wave speed dependence on transmural pressure or spatial location, which concurrently alters vessel compliance, somewhat more striking changes in wave forms were noted in comparison with the SCM. Most apparent among these effects was that, as the wave speed was increased with distance from the ostium (over that used in the standard model), the total volu-

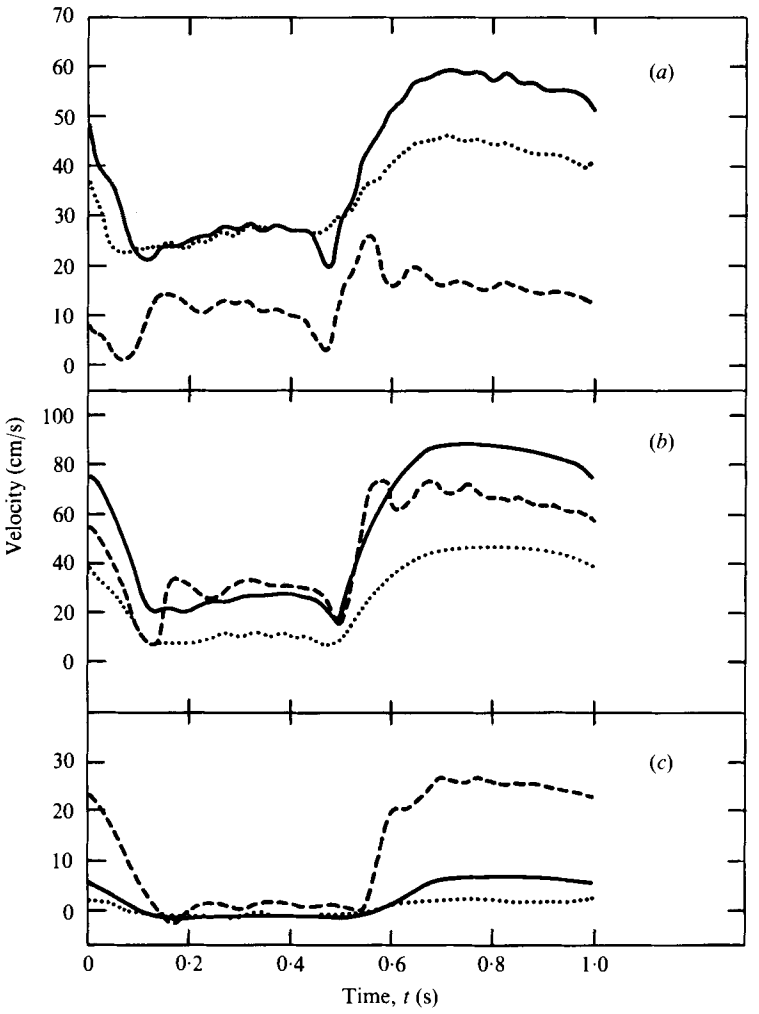

FIGURE 10. Comparison of left coronary artery blood flow velocity at various distances from the left coronary ostium for total geometric scalings of $S_0 = 0{\cdot}2$ cm^2, $S_0 = 0{\cdot}5$ cm^2 and $S_0 = 1{\cdot}5$ cm^2 (standard computer model).

		.....	———	– – – – –
S_0 (cm^2)		0·2	0·5	1·5
z (cm)	(*a*)	0	0	0
	(*b*)	7	12	20
	(*c*)	15	23	40

metric flow at any particular cross-section decreased and the wave oscillation activity during diastole was seen to increase in frequency and decrease in amplitude.

It should be noted that the length of the extramural coronary system, i.e. the distance from the ostium to where the vessels penetrate into the myocardium, is of the order of a quarter-wavelength for a wave with a frequency of 5–10 Hz. This thus suggests that their origin is associated with a wave reflexion process and that this may be initiated during systole, when the extramural vessels are in effect a closed-end tube. Furthermore, although setting the viscosity coefficient equal to zero had a pronounced

effect on the more distal flow rates, little effect was observed on the nature of the flow oscillations with regard to amplitude and frequency. This suggests that these oscillations are basically the result of an inviscid phenomenon. This also is borne out by the syncrony of oscillations simultaneously recorded with a hot-film anemometer velocity probe and an electromagnetic flowmeter.

In considering a possible species dependence of these coronary blood flow oscillations, it was of interest to study the influence of cross-sectional area, vessel taper and system length independently of changes in mechanical parameters. The object here was to examine further the apparent wave reflexion phenomena and the possible effect of cardiac size on the wave oscillation activity. To consider this, the SCM was scaled by a parameter $z' = (S_{0h}/S_0)^{\frac{1}{2}}$, where S_{0h} is the left ostial area for the SCM horse ($S_{0h} = 1{\cdot}5$ cm^2) and S_0 is the left ostial area in the case to be considered. Using this non-dimensional length, all physical length dependences stated explicitly within the standard computer model may be scaled. As an example, a distance stated within the computer program as gz was set equal to gzz'. The length of the system was also scaled, and all other parameters remained unchanged. Boundary conditions were kept equal to those employed in the standard case.

Figure 10 demonstrates the effect of such a scaling on the predicted flow oscillation phenomena for $S_0 = 1{\cdot}5$ cm^2 (SCM), $S_0 = 0{\cdot}5$ cm^2 (a typical pony) and $S_0 = 0{\cdot}2$ cm^2 (a typical human). It should be kept in mind that species differences in end systolic and end diastolic flow rates were not taken into account. For example, in a large horse aortic pressures are nominally 120/100 mm Hg (this was used as input for all cases) while in the human they are about 120/80 mm Hg. Such differences are not reflected in the results in figure 10 as only length-related parameters have been scaled. From these calculations, the amplitude of flow oscillations during diastole is predicted to decrease as S_0 is reduced. Furthermore, as both the area (as scaled by S_0) and the effective length L of the arteries are reduced from horse to approximate human dimensions, the frequency content of the flow oscillations is predicted to increase. Figure 11 demonstrates this frequency dependence on heart size, the results shown being at a fixed length-to-diameter ratio from the left ostium corresponding to 5 cm in the SCM and for both *in vivo* and computer results. The heart size has been scaled through the local cross-sectional area S. This analysis implies that the relative geometric size of the coronary system is one of the most important factors (excluding neural and metabolic changes) in determining the general flow wave form patterns.

Finally, calculations have also been carried out using a linear area–pressure relationship in place of (16). The results obtained in this manner are qualitatively quite similar to those presented here and suggest that studies employing a linear model could be used to obtain better insight into the origin of the low frequency oscillations reported here. Such a linear model could be used to investigate such aspects of the problem as impedance matching and the selective interference and/or superposition of waves. A linear model might also allow a more satisfactory incorporation of vessel branching effects.

In conclusion, a one-dimensional nonlinear mathematical treatment of coronary blood flow in the horse has produced a model that qualitatively, and to a large extent, quantitatively, reproduces many of the more salient features of experimental observations. This model has many empirical aspects to it, and yet quantitative comparisons between *in vivo* coronary flow patterns and corresponding computer calculations at the

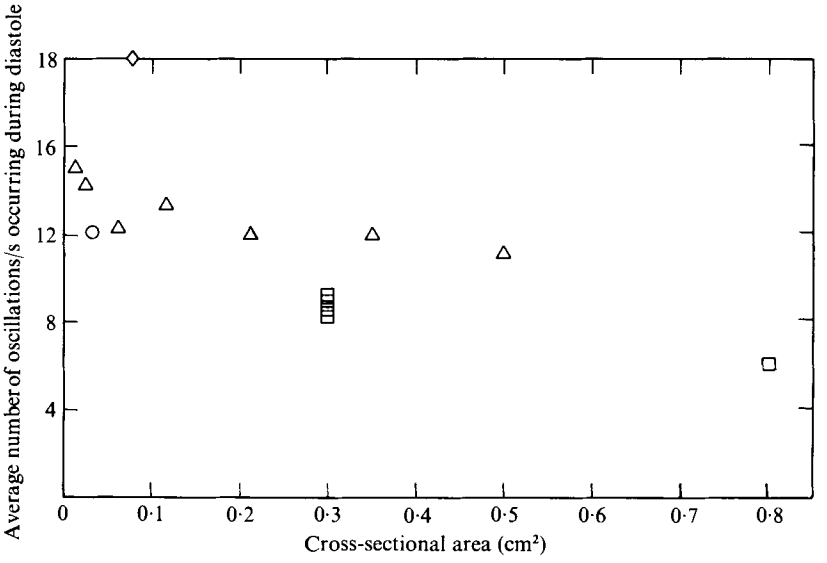

FIGURE 11. Frequency of wave oscillations occurring during diastole from *in vivo* measurements and computer calculations as a function of local cross-sectional area at approximately 5 cm distal to the left coronary ostium. ○, *in vivo* dog (Gregg *et al.*); □, *in vivo* horse; △, computer calculations; ◇, *in vivo* dog.

same vessel position have demonstrated reasonable agreement. In particular, the model correctly predicts volumetric flow rates, fails to reproduce peak flow rates during systole, but during diastole predicts the blood flow patterns quite accurately, including the incidence of a wave oscillation at this time as observed from *in vivo* records. These oscillations are felt to be the result of a wave reflexion process whose nature is not explicitly known. Examination of various mechanical parameters determining coronary blood flow as manifested through the model has revealed that changes in vessel compliance (as modelled by the wave speed c) and in the general cardiac dimensions (as modelled by the length L of the vessels and the left ostium area S_0) are major factors in determining the quantitative nature of any flow oscillations, the resulting blood flow patterns and observed differences in coronary blood flow between individuals as well as between different species.

This investigation was supported by the National Science Foundation under Grant ENG 71-02286.

REFERENCES

ATABEK, H. B., LING, S. C. & PATEL, D. J. 1975 Analysis of coronary flow fields in thoracotomized dogs. *Circ. Res.* **37**, 752–761.

GREGG, D. E., KHOURI, E. M. & RAYFORD, C. R. 1965 Systemic and coronary energetics in the resting unanesthetized dog. *Circ. Res.* **16**, 102–115.

KIRK, E. S. & HONIG, C. R. 1964 An experimental and theoretical analysis of myocardial tissue pressure. *Am. J. Physiol.* **207**, 361–367.

LING, S. C., ATABEK, H. B., LETZING, W. G. & PATEL, D. J. 1973 Nonlinear analysis of aortic flow in living dogs. *Circ. Res.* **33**, 198–212.

LISTER, J. 1960 The numerical solution of hyperbolic differential equations by the method of characteristics. In *Mathematics for Digital Computers*, pp. 76–91. McGraw-Hill.

McDonald, D. A. 1974 *Blood Flow in Arteries.* 2nd edn. London: Edward Arnold.

Nerem, R. M., Rumberger, J. A., Gross, D. R., Muir, W. W. & Geiger, G. L. 1976 Hot film coronary artery velocity measurements in horses. *Cardiovasc. Res.* **3**, 301–313.

Randall, R. T. & Armour, T. J. 1971 Canine left ventricular intramyocardial pressures. *Am. J. Physiol.* **220**, 1833–1839.

Rockwell, R. L. 1969 Nonlinear analysis of pressure and shock waves in blood vessels. Ph.D. dissertation, Stanford University.

Rubio, R. & Berne, R. M. 1975 Regulation of coronary blood flow. *Prog. Cardiovasc. Dis.* **18**, 105–122.

Rumberger, J. A., Nerem, R. M. & Muir, W. W. 1977 Phasic pressure and wave transmission characteristics in the coronary arteries of the horse. Submitted to *Cardiovasc. Res.*

Van der Werff, T. 1974 Significant parameters in arterial pressure and velocity development. *J. Biomech.* **7**, 437–450.

Wells, M. K., Winter, D. C., Nelson, A. W. & McCarthy, T. C. 1975 Blood velocity patterns in coronary arteries. *Trans. A.S.M.E. J. Biomech. Engng* **1**, 26–32.

Womersley, J. R. 1957 Elastic tube theory of pulse transmission and oscillatory flow in mammalian arteries. *Wright Air Development Center, Dayton, Ohio, Tech. Rep.* WADC-TR, 56–614.